

CERN-TH/95-241

JINR-E2-95-110

Pair Production in Small-Angle Bhabha Scattering

A.B. Arbuzov, E.A. Kuraev

Bogoliubov Laboratory of Theoretical Physics, JINR,
Dubna, 141980, Russia

N.P. Merenkov

Physico-Technical Institute, Kharkov, 310108, Ukraine

and

L. Trentadue ^{1, 2}

Theoretical Physics Division, CERN,
CH-1211 Geneva 23, Switzerland

Abstract

Radiative corrections due to the production of virtual as well as real soft and hard pairs in small-angle Bhabha scattering are calculated analytically. Both the collinear and the semi-collinear kinematical regions of hard pair production are considered. The calculation, within the leading and next-to-leading logarithmic approximation, provides an accuracy of $O(0.1\%)$. Numerical results show that the effects of pair production have to be taken into account for a luminosity determination accurate to $O(0.1\%)$ at LEP.

CERN-TH/95-241

September 1995

¹On leave of absence from the Dipartimento di Fisica, Università di Parma, Parma, Italy.

²INFN, Gruppo Collegato di Parma, Sezione di Milano, Milano, Italy.

1 Introduction

The electron–positron scattering process (Bhabha process) at small angles is used for the measurement of the luminosity at LEP I [1]. This technique provides an experimental accuracy of the $O(0.1\%)$, or even better [2]. Such an accurate theoretical calculation of the Bhabha cross-section was missing [3]. Recently [4] the radiative corrections due to the emission of virtual, real soft and hard photons and pairs have been calculated up to the three loop providing an $O(0.1\%)$ accurate cross-section. In this work [4] we gave the results of the performed analytical calculations. The leading ($\sim (\alpha L/\pi)^{1,2,3}$) contributions as well as the next to leading ($\sim \alpha/\pi, (\alpha/\pi)^2 L$) ones were calculated explicitly for the processes with the emission of photons where $L = \ln Q^2/m_e^2$ and $Q^2 \sim 10 (\text{GeV}/c)^2$ is the squared momentum transferred. For a given scattering angle θ one has $Q^2 = 2\epsilon^2(1 - \cos \theta)$ with ϵ the beam energy. Also the pair production processes and the contributions due to the emission of virtual, soft and real hard pairs were considered. However, the production of real hard pairs was calculated only in the collinear kinematics (CK) limit [4]. In order to assess the accuracy already obtained within the collinear limit, in this paper, we carry a systematic study of the hard pair emission within the semi-collinear kinematics (SCK). We present also the total contribution to the observable Bhabha cross-section due to the pair production

$$e^-(p_1) + e^+(p_2) \rightarrow e^-(q_1) + e^+(q_2) + e^-(p_-) + e^+(p_+), \quad (1)$$

which takes into account the cuts on the detection of the scattered electron and positron. We accept the convention [1–3] to consider as an event of the Bhabha process one in which the angles of the simultaneously registered particles hitting the opposite detectors lay in the range:

$$\theta_{\min} < \theta_e < \theta_{\max} = \rho\theta_{\min}, \quad \pi - \rho\theta_{\min} < \theta_{\bar{e}} < \pi - \theta_{\min}, \quad (2)$$

($\theta_{\min} \sim 3^\circ$, $\rho \gtrsim 1$) with respect to the beam direction. The second condition is imposed on the energy fractions of the scattered electron and positron:

$$x_e x_{\bar{e}} > x_c, \quad x_{e,\bar{e}} = 2\varepsilon_{e,\bar{e}}/\sqrt{s}, \quad s = 4\varepsilon^2, \quad (3)$$

where ε is the energy of the initial electron (or positron), $\varepsilon_{e,(\bar{e})}$ is the energy of the scattered electron (positron)³.

Our method for the real hard pair production cross-section calculation within the logarithmic accuracy consists in the separation of the contributions due to the collinear and semi-collinear kinematical regions [5,6]. In the

³Here and in the following, it is implied that the centre of mass is the reference frame.

first one (CK) we suggest that both electron and positron from the created pair go in the narrow cone along to the direction of one of the charged particles (the projectile (scattered) electron \vec{p}_1 (\vec{q}_1) or the projectile (scattered) positron \vec{p}_2 (\vec{q}_2)):

$$\widehat{\vec{p}_+\vec{p}_-} \sim \widehat{\vec{p}_-\vec{p}_i} \sim \widehat{\vec{p}_+\vec{p}_i} < \theta_0 \ll 1, \quad \varepsilon\theta_0/m \gg 1, \quad \vec{p}_i = \vec{p}_1, \vec{p}_2, \vec{q}_1, \vec{q}_2. \quad (4)$$

The contribution of the CK contains terms of the order of $(\alpha L/\pi)^2$ and $(\alpha\pi)^2 L$. In the semi-collinear region only one of conditions (4) on the angles is fulfilled:

$$\begin{aligned} \widehat{\vec{p}_+\vec{p}_-} < \theta_0, \quad \widehat{\vec{p}_\pm\vec{p}_i} > \theta_0; \quad \text{or} \quad \widehat{\vec{p}_-\vec{p}_i} < \theta_0, \quad \widehat{\vec{p}_+\vec{p}_i} > \theta_0; \\ \text{or} \quad \widehat{\vec{p}_-\vec{p}_i} > \theta_0, \quad \widehat{\vec{p}_+\vec{p}_i} < \theta_0. \end{aligned} \quad (5)$$

The contribution of the SCK contains the terms of the form:

$$\left(\frac{\alpha}{\pi}\right)^2 L \ln \frac{\theta_0}{\theta}, \quad \left(\frac{\alpha}{\pi}\right)^2 L, \quad (6)$$

where $\theta = \widehat{\vec{p}_-\vec{q}_1}$ is the scattering angle. The auxiliary parameter θ_0 disappears in the total sum of the CK and SCK contributions. We systematically omit the terms without large logarithms; they are of the form $(\alpha/\pi)^2 \cdot \text{const} \sim 10^{-5}$.

We restrict ourselves to the case when the electron–positron pair is created. The effects due to the other pair creation ($\mu^+\mu^-$, $\pi^+\pi^-$, etc.) are at least one order of magnitude smaller and can be neglected, as will be seen from the numerical analysis. All possible mechanisms for pair creation (the singlet and non-singlet ones) as well as the identity of the particles in the final state are taken into account. In the case of small-angle Bhabha scattering, only the scattering-type diagrams are relevant among the the total 36 Feynman tree level diagrams. Besides, we are convinced of the cancellations of the interference between the amplitudes describing the production of pairs moving along the electron direction and the positron one known as up–down cancellation.

The sum of the contributions due to the virtual pair emission (due to the vacuum polarization insertions in the virtual photon Green function) and of those due to the real soft pair emission does not contain cubic ($\sim L^3$) terms, but depends on the auxiliary parameter $\Delta = \delta\varepsilon/\varepsilon$ ($m_e \ll \delta\varepsilon \ll \varepsilon$, ε is the energy sum of the soft pair components). The Δ -dependence disappears in the total sum after adding the contributions due to the real hard pair production. Before summing one has to integrate the hard pair contributions over the energy fractions of pair components as well as over the ones of the scattered electron and positron:

$$\begin{aligned} \Delta &= \frac{\delta\varepsilon}{\varepsilon} < x_1 + x_2, & x_c < x = 1 - x_1 - x_2 < 1 - \Delta, \\ x_1 &= \frac{\varepsilon_+}{\varepsilon}, & x_2 &= \frac{\varepsilon_-}{\varepsilon}, & x &= \frac{q_1^0}{\varepsilon}, \end{aligned} \quad (7)$$

where ε_{\pm} are the energies of the positron and electron from the created pair. We consider for definiteness the case where the created hard pair moves close to the direction of the initial (or scattered) electron.

The paper is organized as follows: in the second part we consider the emission of the hard pair in the collinear kinematics. The results turned out to be very close to the ones obtained by one of us (N.P.M.) in paper [6] for the case of the pair production in electron–nuclei scattering and applied to the case of small-angle Bhabha scattering in [4]. For completeness, we present very briefly the derivation and give the result correcting some misprints in [6]. In the third part we consider the semi-collinear kinematical regions. The differential cross-section is obtained there and integrated over the angles and energy fractions of the pair components. In the fourth part we give the expression of the radiative corrections to the experimental cross-section due to pair production. The results are illustrated numerically in tables and discussed in the Conclusions.

2 The Collinear Kinematics

In evaluating the cross-section we see that there are four different CK regions: when the created pair goes along the direction of the initial (scattered) electron or positron [4]. We will consider only two of them, corresponding to the initial and the final electron directions. For the case of the pair emission along the initial electron, it is useful to decompose the particle momenta into the longitudinal and transverse components:

$$\begin{aligned} p_+ &= x_1 p_1 + p_+^{\perp}, & p_- &= x_2 p_1 + p_-^{\perp}, & q_1 &= x p_1 + q_1^{\perp}, \\ x &= 1 - x_1 - x_2, & q_2 &\approx p_2, & p_+^{\perp} + p_-^{\perp} + q_1^{\perp} &= 0, \end{aligned} \quad (8)$$

where p_i^{\perp} are the transverse two-dimensional momenta of the final particles with respect to the initial electron beam direction. It is convenient to introduce the following dimensionless quantities for the relevant kinematical invariants:

$$\begin{aligned} z_i &= \left(\frac{\varepsilon\theta_i}{m}\right)^2, & z_1 &= \left(\frac{p_-^{\perp}}{m}\right)^2, & z_2 &= \left(\frac{p_+^{\perp}}{m}\right)^2, & 0 < z_i < \left(\frac{\varepsilon\theta_0}{m}\right)^2 \gg 1, & (9) \\ A &= \frac{(p_+ + p_-)^2}{m^2} = (x_1 x_2)^{-1} [(1-x)^2 + x_1^2 x_2^2 (z_1 + z_2 - 2\sqrt{z_1 z_2} \cos\phi)], \\ A_1 &= \frac{2p_1 p_-}{m^2} = x_2^{-1} [1 + x_2^2 + x_2^2 z_2], & A_2 &= \frac{2p_1 p_+}{m^2} = x_1^{-1} [1 + x_1^2 + x_1^2 z_1], \\ C &= \frac{(p_1 - p_-)^2}{m^2} = 2 - A_1, & D &= \frac{(p_1 - q_1)^2}{m^2} - 1 = A - A_1 - A_2, \end{aligned}$$

where ϕ is the azimuthal angle between the planes $(\vec{p}_1 p_-^{\perp})$ and $(\vec{p}_1 p_+^{\perp})$.

Keeping only the terms from the squared matrix element module summed over the spin states module that give non zero contribution to the cross-section in the limit $\theta_0 \rightarrow 0$, we find that only 8 of the 36 tree level Feynman diagrams are essential. They are drawn in fig. 1.

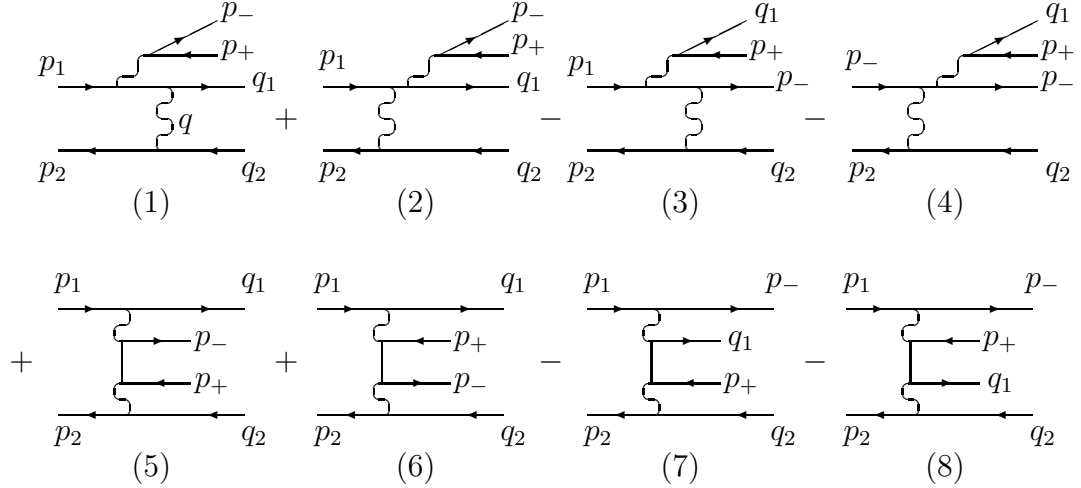


Fig. 1. The Feynman diagram giving logarithmically enhanced contributions in the kinematical region where the created pair goes along the electron direction. The signs represent the Fermi–Dirac statistics of the interchanged fermions.

The result has the factorized form (in agreement with the factorization theorem [8]):

$$\sum_{\text{spins}} |M|^2 \Big|_{p_+, p_- \parallel p_1} = \sum_{\text{spins}} |M_0|^2 2^7 \pi^2 \alpha^2 \frac{I}{m^4}, \quad (10)$$

where one of the factors corresponds to the matrix element in the Born approximation (without pair production):

$$\sum_{\text{spins}} |M_0|^2 = 2^7 \pi^2 \alpha^2 \left(\frac{s^4 + t^4 + u^4}{s^2 t^2} \right), \quad (11)$$

$$s = 2p_1 p_2 x, \quad t = -Q^2 x, \quad u = -s - t,$$

and the quantity I , the collinear factor, coincides with the expression for I_a obtained in paper [6]. We put it here in terms of our kinematical variables:

$$I = (1 - x_2)^{-2} \left(\frac{A(1 - x_2) + Dx_2}{DC} \right)^2 + (1 - x)^{-2} \left(\frac{C(1 - x) - Dx_2}{AD} \right)^2$$

$$+ \frac{1}{2xAD} \left[\frac{2(1 - x_2)^2 - (1 - x)^2}{1 - x} + \frac{x_1 x - x_2}{1 - x_2} + 3(x_2 - x) \right]$$

$$\begin{aligned}
& + \frac{1}{2xCD} \left[\frac{(1-x_2)^2 - 2(1-x)^2}{1-x_2} + \frac{x-x_1x_2}{1-x} + 3(x_2-x) \right] \\
& + \frac{x_2(x^2+x_2^2)}{2x(1-x_2)(1-x)AC} + \frac{3x}{D^2} + \frac{2C}{AD^2} + \frac{2A}{CD^2} + \frac{2(1-x_2)}{xA^2D} \\
& - \frac{4C}{xA^2D^2} - \frac{4A}{D^2C^2} + \frac{1}{DC^2} \left[\frac{(x_1-x)(1+x_2)}{x(1-x_2)} - 2\frac{1-x}{x} \right]. \tag{12}
\end{aligned}$$

Rearranging the phase volume of the final particles as follows:

$$\begin{aligned}
d\Gamma &= \frac{d^3q_1 d^3q_2}{(2\pi)^6 2q_1^0 2q_2^0} (2\pi)^4 \delta^4(p_1x + p_2 - q_1 - q_2) \tag{13} \\
&\times m^4 2^{-8} \pi^{-4} x_1 x_2 dx_1 dx_2 dz_1 dz_2 \frac{d\phi}{2\pi},
\end{aligned}$$

and integrating over the variables of the created pair, we obtain (see Appendix A):

$$\begin{aligned}
\bar{I} &= \int_0^{2\pi} \frac{d\phi}{2\pi} \int_0^{z_0} dz_1 \int_0^{z_0} dz_2 I = \frac{L_0}{2xx_1x_2} \left\{ D_1 \left(L_0 + 2 \ln \frac{x_1x_2}{x} \right) \right. \tag{14} \\
&+ \left. D_2 \ln \frac{(1-x_2)(1-x)}{xx_2} + D_3 \right\}, \quad L_0 = \ln \left(\frac{\varepsilon\theta_0}{m} \right)^2, \\
D_1 &= 2xx_1x_2 \left(\frac{1}{(1-x)^4} + \frac{1}{(1-x_2)^4} \right) - \frac{(1-x_2)^2}{(1-x)^2} - \frac{(1-x)^2}{(1-x_2)^2} + 1 \\
&+ \frac{(x+x_2)^2}{2(1-x)(1-x_2)} + \frac{3(x_2-x)^2}{2(1-x)(1-x_2)} - \frac{x^2+x_2^2}{(1-x)(1-x_2)} \\
&- 2xx_2 \left(\frac{1}{(1-x)^2} + \frac{1}{(1-x_2)^2} \right), \quad D_2 = \frac{2(x^2+x_2^2)}{(1-x)(1-x_2)}, \\
D_3 &= \frac{2xx_1x_2}{(1-x_2)^2} \left(-\frac{8}{(1-x_2)^2} + \frac{(1-x)^2}{xx_1x_2} \right) + \frac{2xx_1x_2}{(1-x)^2} \left[\frac{x_2}{xx_1} \right. \\
&+ \left. \frac{2(x_1-x_2)}{xx_1(1-x)} - \frac{8}{(1-x)^2} + \frac{1}{xx_1x_2} - \frac{4}{x(1-x)} \right] + 6 + 4x \left[\frac{x_2-x_1}{(1-x)^2} \right. \\
&- \left. \frac{x_1}{x(1-x)} \right] + \frac{4(xx_2-x_1)}{(1-x_2)^2} - \frac{4(1-x_2)x_1x_2}{(1-x)^3} + \frac{8xx_1x_2^2}{(1-x)^4} \\
&- \frac{xx_2^2}{(1-x_2)^4} + \frac{x_2}{(1-x_2)^2} \left[4(1-x) + \frac{2(x-x_1)(1+x_2)}{1-x_2} \right].
\end{aligned}$$

By doing the same also in the case of a pair moving in the direction of the scattered electron, integrating the obtained sum over the energy fractions of the pair components, and finally adding the contribution of the two remaining

CK regions (when the pair goes along the positron direction) we obtain:

$$\begin{aligned}
d\sigma_{\text{coll}} &= \frac{\alpha^4 dx}{\pi Q_1^2} \int \frac{\rho^2 dz}{z^2} L \left\{ R_0(x) \left(L + 2 \ln \frac{\lambda^2}{z} \right) (1 + \Theta) \right. \\
&\quad \left. + 4R_0(x) \ln x + 2\Theta f(x) + 2f_1(x) \right\}, \quad \lambda = \frac{\theta_0}{\theta_{\min}}, \\
\Theta &\equiv \Theta(x^2 \rho^2 - z) = \begin{cases} 1, & x^2 \rho^2 > z, \\ 0, & x^2 \rho^2 \leq z, \end{cases} \\
R_0(x) &= \frac{2}{3} \frac{(1+x^2)}{1-x} + \frac{(1-x)}{3x} (4 + 7x + 4x^2) + 2(1+x) \ln x, \\
f(x) &= -\frac{107}{9} + \frac{136}{9}x - \frac{2}{3}x^2 - \frac{4}{3x} - \frac{20}{9(1-x)} + \frac{2}{3}[-4x^2 - 5x + 1 \\
&\quad + \frac{4}{x(1-x)}] \ln(1-x) + \frac{1}{3}[8x^2 + 5x - 7 - \frac{13}{1-x}] \ln x - \frac{2}{1-x} \ln^2 x \\
&\quad + 4(1+x) \ln x \ln(1-x) - \frac{2(3x^2-1)}{1-x} \text{Li}_2(1-x), \\
f_1(x) &= -x \Re f\left(\frac{1}{x}\right) = -\frac{116}{9} + \frac{127}{9}x + \frac{4}{3}x^2 + \frac{2}{3x} - \frac{20}{9(1-x)} + \frac{2}{3}[-4x^2 \\
&\quad - 5x + 1 + \frac{4}{x(1-x)}] \ln(1-x) + \frac{1}{3}[8x^2 - 10x - 10 + \frac{5}{1-x}] \ln x \\
&\quad - (1+x) \ln^2 x + 4(1+x) \ln x \ln(1-x) - \frac{2(x^2-3)}{1-x} \text{Li}_2(1-x), \\
\text{Li}_2(x) &\equiv -\int_0^x \frac{dy}{y} \ln(1-y), \quad Q_1 = \varepsilon \theta_{\min}, \quad L = \ln \frac{z Q_1^2}{m^2},
\end{aligned} \tag{15}$$

Some misprints in the expressions for $f(x)$ and $f_1(x)$ in [4,6] are corrected here.

3 The Semi-Collinear Kinematics

We will restrict ourselves again to the case when the created pair goes close to the electron momentum (the initial or final one). Analogous considerations can be made in the CM system in the case when the pair follows the positron momentum. There are three different semi-collinear regions, which contribute to the cross-section within the required accuracy of $O(0.1\%)$. The first region includes the events with a very small invariant mass of the created pair:

$$4m^2 \ll (p_+ + p_-)^2 \ll |q^2|,$$

when the pair escapes the narrow cones (defined by θ_0) along both the projectile and the scattered electron momentum directions. We represent this

semi-collinear kinematics (SCK) region with the notation $\vec{p}_+ \parallel \vec{p}_-$. Only the diagrams in fig. 1(1) and fig. 1(2) do contribute to this region and this is because of the smallness of the virtuality of the pair producing photon.

The second SCK region includes the events where the invariant mass of the created positron and the scattered electron is small: $4m^2 \ll (p_+ + q_1)^2 \ll |q^2|$, with the restriction that the positron should escape the narrow cone along the initial electron momentum direction. We represent it by $\vec{p}_+ \parallel \vec{q}_1$ and note that only two diagrams fig. 1(3) and fig. 1(4), contribute here.

The third SCK region includes the events when the created electron goes inside the narrow cone along the initial electron momentum direction but the created positron does not. We represent it by $\vec{p}_- \parallel \vec{p}_1$. Only the diagrams fig. 1(7) and fig. 1(8) are relevant here.

The differential cross-section takes the following form:

$$\begin{aligned} d\sigma &= \frac{\alpha^4}{8\pi^4 s^2} \frac{|M|^2}{q^4} \frac{dx_1 dx_2 dx}{x_1 x_2 x} d^2 p_+^\perp d^2 p_-^\perp d^2 q_1^\perp d^2 q_2^\perp \delta(1 - x_1 - x_2 - x) \quad (16) \\ &\times \delta^{(2)}(p_+^\perp + p_-^\perp + q_1^\perp + q_2^\perp), \quad |M|^2 = -L_{\lambda\rho} p_{2\lambda} p_{2\rho}, \end{aligned}$$

where x_1 (x_2), x and p_+^\perp (p_-^\perp), q_1^\perp are the energy fractions and the perpendicular momenta of the created positron (electron) and the scattered electron respectively; $s = (p_1 + p_2)^2$ and $q^2 = -Q^2 = (p_2 - q_2)^2 = -\varepsilon^2 \theta^2$ are the centre-of-mass energy squared and the squared momentum transferred; the leptonic tensor $L_{\lambda\rho}$ has different forms for different SCK regions.

3.1 $\vec{p}_+ \parallel \vec{p}_-$ region

For the region of small $(p_+ + p_-)^2$ we can use the leptonic tensor obtained in paper [6]. Keeping only the relevant terms, we present it in the form:

$$\begin{aligned} \frac{P^4}{8} L_{\lambda\rho} &= \frac{4P^2 q^2}{(1)(2)} [-(p_1 p_1)_{\lambda\rho} - (q_1 q_1)_{\lambda\rho} + (p_1 q_1)_{\lambda\rho}] \\ &- 4(p_+ p_-)_{\lambda\rho} \left(1 - \frac{q^2 P^2}{(1)(2)}\right) - \frac{4}{(1)} [q^2 (p_1 q_1)_{\lambda\rho} - 2(p_1 p_+) (q_1 p_-)_{\lambda\rho} \\ &- 2(p_1 p_-) (q_1 p_1)_{\lambda\rho}] - \frac{4}{(2)} [P^2 (p_1 q_1)_{\lambda\rho} - 2(p_+ q_1) (p_1 p_-)_{\lambda\rho} \\ &- 2(p_- q_1) (p_1 p_+)_{\lambda\rho}] - \frac{32(p_1 p_+) (p_1 p_-)}{(1)^2} (q_1 q_1)_{\lambda\rho} - \frac{32(q_1 p_+) (q_1 p_-)}{(2)^2} (p_1 p_1)_{\lambda\rho} \\ &+ \frac{8(p_1 q_1)_{\lambda\rho}}{(1)(2)} [P^2 (p_1 q_1) - 2(p_1 p_+) (p_- q_1) - 2(p_1 p_-) (q_1 p_+)], \quad (17) \end{aligned}$$

where

$$P = p_+ + p_-, \quad (aa)_{\lambda\rho} = a_\lambda a_\rho, \quad (ab)_{\lambda\rho} = a_\lambda b_\rho + a_\rho b_\lambda,$$

$$q = p_1 - q_1 - P, \quad (1) = (p_1 - P)^2 - m^2, \quad (2) = (p_1 - q)^2 - m^2.$$

After some algebraic transformations the expression for $|M|^2$ entering the cross-section can be put in the form:

$$\begin{aligned} \frac{1}{q^4}|M|^2 &= -\frac{2s^2}{q^4P^4} \left\{ -\frac{4P^2q^2}{(1)(2)} [(1-x_1)^2 + (1-x_2)^2] \right. \\ &\quad \left. + \frac{128}{(1)^2(2)^2} [(q_1p)(p_+p_1) - x(p_1p)(q_1p_+)]^2 \right\}, \end{aligned} \quad (18)$$

where $p = p_- - x_2p_+/x_1$, $(q_2^\perp)^2 = -q^2$. In the considered region we can use the relations

$$(1) = -\frac{1-x}{x_1} 2(p_1p_+), \quad (2) = \frac{1-x}{x_1} 2(q_1p_+). \quad (19)$$

It is useful to represent all invariants in terms of the Sudakov variables (energy fractions and perpendicular momenta), namely

$$\begin{aligned} q_1^2 &= \frac{1}{x_1x_2} ((p^\perp)^2 + m^2(1-x)^2), \quad 2(q_1p_+) = \frac{1}{xx_1} (xp_+^\perp - x_1q_1^\perp)^2, \quad (20) \\ 2(p_1p_+) &= \frac{1}{x_1} (p_+^\perp)^2, \quad 2(p_1p) = \frac{2}{x_1^2} p^\perp p_+^\perp, \quad 2(q_1p) = \frac{2}{x_1^2} (p^\perp [xp_+^\perp - x_1q_1^\perp]), \\ p^\perp &= x_1p_-^\perp - x_2p_+^\perp. \end{aligned}$$

The large logarithm appears in the cross-section after the integration over p^\perp . In order to carry out this integration we can use the relation

$$\delta^{(2)} d^2p_+^\perp d^2p_-^\perp = \frac{1}{(1-x)^2} d^2p^\perp, \quad (21)$$

which is valid in the region $\vec{p}_+ \parallel \vec{p}_-$. After the integration we derive the contribution of the first SCK region to the cross-section:

$$\begin{aligned} d\sigma_{\vec{p}_+ \parallel \vec{p}_-} &= \frac{\alpha^4}{\pi} L dx dx_2 \frac{d(q_2^\perp)^2}{(q_2^\perp)^2} \cdot \frac{d(q_1^\perp)^2}{(q_1^\perp + q_2^\perp)^2} \\ &\quad \times \frac{d\phi}{2\pi} \cdot \frac{1}{(q_1^\perp + xq_2^\perp)^2} \left[(1-x_1)^2 + (1-x_2)^2 - \frac{4xx_1x_2}{(1-x)^2} \right], \end{aligned} \quad (22)$$

where ϕ is the angle between the two dimensional vectors q_1^\perp and q_2^\perp .

At this stage it is necessary to use the restrictions on the two dimensional momenta q_1^\perp and q_2^\perp . They appear when the contribution of the CK region (which in this case represents the narrow cones with the opening angle θ_0 along the momentum directions of both initial and scattered electron) is excluded.

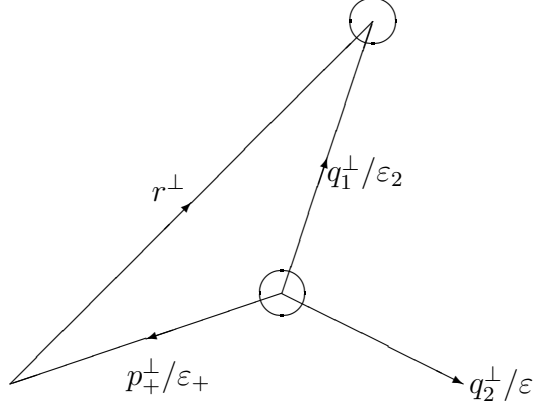


Fig. 2. The kinematics of an event in the angular perpendicular plane corresponding to the SCK region $\vec{p}_+ \parallel \vec{p}_-$.

The kinematics of the events corresponding to the region $\vec{p}_+ \parallel \vec{p}_-$ in the perpendicular plane is shown in fig. 2. The circles radius θ_0 represent in the figure the forbidden collinear regions. The elimination of those regions gives the following restrictions:

$$\left| \frac{p_+^\perp}{\epsilon_+} \right| > \theta_0, \quad |r^\perp| = \left| \frac{p_+^\perp}{\epsilon_+} - \frac{q_1^\perp}{\epsilon_2} \right| > \theta_0, \quad (23)$$

where ϵ_+ and ϵ_2 are the energies of the created positron and of the scattered electron respectively. In order to exclude p_+^\perp from the above equation we use the conservation of the perpendicular momentum in the region $p_+ \parallel \vec{p}_-$:

$$q_1^\perp + q_2^\perp + \frac{1-x}{x_1} p_+^\perp = 0. \quad (24)$$

It is useful to introduce the dimensionless variables $z_{1,2} = (q_{1,2}^\perp)^2 / (\epsilon \theta_{\min})^2$, where θ_{\min} is the minimal angle at which the scattered particles (electron and positron) are recorded by the detector. Here we consider only the symmetrical circular detectors. The conditions (23) can be rewritten as follows:

$$\begin{cases} 1 > \cos \phi > -1 + \frac{\lambda^2(1-x)^2 - (\sqrt{z_1} - \sqrt{z_2})^2}{2\sqrt{z_1 z_2}}, & |\sqrt{z_1} - \sqrt{z_2}| < \lambda(1-x), \\ 1 > \cos \phi > -1, & |\sqrt{z_1} - \sqrt{z_2}| > \lambda(1-x), \quad \lambda = \theta_0/\theta_{\min}, \end{cases} \quad (25)$$

$$\begin{cases} 1 > \cos \phi > -1 + \frac{\lambda^2 x^2 (1-x)^2 - (\sqrt{z_1} - x\sqrt{z_2})^2}{2x\sqrt{z_1 z_2}}, & |\sqrt{z_1} - x\sqrt{z_2}| < \lambda x(1-x), \\ 1 > \cos \phi > -1, & |\sqrt{z_1} - x\sqrt{z_2}| > \lambda x(1-x). \end{cases} \quad (26)$$

The restrictions in eq.(25)[(26)] exclude the phase space, corresponding to the narrow cone along the direction of the initial [scattered] electron.

The conditions of the LEP I experiment are:

$$\theta_0 \gg \frac{m}{\varepsilon} \approx 10^{-5} \quad \text{and} \quad \theta_{\min} \sim 10^{-2}. \quad (27)$$

This is the reason for considering $\lambda \ll 1$. The procedure of integration of the differential cross-section over regions (25) and (26) is described in detail in Appendix B. Here we give the contribution of the SCK region $\vec{p}_+ \parallel \vec{p}_-$ to the cross-section provided that only the scattered electrons with the energy fraction x exceeding x_c could be recorded:

$$\begin{aligned} \sigma_{\vec{p}_+ \parallel \vec{p}_-} &= \frac{\alpha^4}{\pi Q_1^2} \mathcal{L} \int_1^{\rho^2} \frac{dz}{z^2} \int_{x_c}^{1-\Delta} dx \int_0^{1-x} dx_2 \left[\frac{(1-x_1)^2 + (1-x_2)^2}{(1-x)^2} \right. \\ &\quad \left. - \frac{4xx_1x_2}{(1-x)^2} \right] \left\{ (1+\Theta) \ln \frac{z}{\lambda^2} + \Theta \ln \frac{(x^2\rho^2 - z)^2}{x^2(x\rho^2 - z)^2} \right. \\ &\quad \left. + \ln \left| \frac{(z-x^2)(\rho^2 - z)(z-1)}{(z-x)^2(z-x^2\rho^2)} \right| \right\}, \quad \mathcal{L} = \ln \frac{\varepsilon^2 \theta_{\min}^2}{m^2}, \quad (28) \end{aligned}$$

where $Q_1^2 = \varepsilon^2 \theta_{\min}^2$, $\rho = \theta_{\max}/\theta_{\min}$ (θ_{\max} is the maximal angle of the final particle registration), $\Theta \equiv \Theta(x^2\rho^2 - z)$, $z \equiv z_2$. The auxiliary parameter Δ entering eq. (28) defines the minimal energy of the created hard pair: $2m/\varepsilon \ll \Delta \ll 1$. Note that we replaced L by \mathcal{L} because we do make no difference between them at the single logarithmic level.

3.2 $\vec{p}_+ \parallel \vec{q}_1$ region

As was already mentioned, in the SCK region $\vec{p}_+ \parallel \vec{q}_1$ only diagrams fig. 1(3) and fig. 1(4) contribute. The leptonic tensor could in this case be derived from eq. (17) by the substitution $p_- \leftrightarrow q_1$, and the squared matrix element could be written as

$$\begin{aligned} |M|_{\vec{p}_+ \parallel \vec{q}_1}^2 &= -\frac{4s^2}{q_1'^2 \vec{q}_2'^2} \cdot \frac{1}{(1')(2)} \left\{ (1-x_1)^2 + (1-x_2)^2 \right. \\ &\quad \left. + \frac{32}{q_1'^2 \vec{q}_2'^2} \cdot \frac{1}{(1')(2)} [(p_1 p_+)(p_- p') - x_2(p_- p_+)(p_1 p')]^2 \right\}, \quad (29) \end{aligned}$$

where

$$\begin{aligned} p' &= q_1 - p_+ x/x_1, & q_1'^2 &= (q_1 + p_+)^2, \\ (2) &= 2(p_+ p_-)(1-x_2)/x_1, & (1') &= -2(p_1 p_+)(1-x_2)/x_1. \end{aligned}$$

The integration of the matrix element over $(p_1^\perp)^2$ and $(p_2^\perp)^2$ could be carried out analogously to the previous case, and the contribution of the $\vec{p}_+ \parallel \vec{q}_1$ region could be presented in the following form:

$$\begin{aligned} d\sigma_{\vec{p}_+ \parallel \vec{q}_1} &= \frac{\alpha^4}{\pi} L dx dx_2 \frac{d(q_2^\perp)^2}{(q_2^\perp)^2} \cdot \frac{d(q_1^\perp)^2}{(q_1^\perp)^2} \\ &\times \frac{d\phi}{2\pi} \cdot \frac{1}{(q_1^\perp + xq_2^\perp)^2} \cdot \frac{x^2}{(1-x_2)^2} \left[\frac{(1-x)^2 + (1-x_1)^2}{(1-x_2)^2} - \frac{4xx_1x_2}{(1-x_2)^2} \right]. \end{aligned} \quad (30)$$

The restriction on the phase space, coming from the exclusion of the collinear region when the created pair flies inside the narrow cone along the scattered electron, leads to the relation:

$$\left| \frac{p_-^\perp}{\varepsilon_-} - \frac{q_1^\perp}{\varepsilon_2} \right| > \theta_0. \quad (31)$$

In eq. (31) we have to exclude p_-^\perp using the conservation of the perpendicular momentum in the case under consideration: $p_-^\perp + q_2^\perp + q_1^\perp(1-x_2)/x = 0$. In terms of the dimensionless variables z_1 , z_2 and the angle ϕ , eq. (31) could be rewritten as

$$\begin{cases} 1 > \cos \phi > -1 + \frac{\lambda^2 x^2 x_2^2 - (\sqrt{z_1} - x\sqrt{z_2})^2}{2x\sqrt{z_1 z_2}}, & |\sqrt{z_1} - x\sqrt{z_2}| < \lambda x x_2, \\ 1 > \cos \phi > -1, & |\sqrt{z_1} - x\sqrt{z_2}| > \lambda x x_2. \end{cases} \quad (32)$$

The integration of the differential cross-section (30) over the region defined in eq. (32) leads to the following result for the contribution of the $\vec{p}_+ \parallel \vec{q}_1$ SCK region:

$$\begin{aligned} \sigma_{\vec{p}_+ \parallel \vec{q}_1} &= \frac{\alpha^4}{\pi Q_1^2} \mathcal{L} \int_1^{\rho^2} \frac{dz}{z^2} \int_{x_c}^{1-\Delta} dx \int_0^{1-x} dx_2 \left[\frac{(1-x)^2 + (1-x_1)^2}{(1-x_2)^2} \right. \\ &\quad \left. - \frac{4xx_1x_2}{(1-x_2)^4} \right] \left\{ \ln \frac{z}{\lambda^2} + \ln \frac{(\rho^2 - z)(z - 1)}{x_2^2 \rho^2} \right\}. \end{aligned} \quad (33)$$

3.3 $\vec{p}_- \parallel \vec{p}_1$ region

In the SCK region $\vec{p}_- \parallel \vec{p}_1$, only diagrams fig. 1(7) and fig. 1(8) contribute to the cross-section within the required accuracy. In this case, the leptonic tensor could be derived from eq. (17) by the substitution $p_1 \leftrightarrow -p_+$, and the squared matrix element has the form:

$$\begin{aligned} |M|_{\vec{p}_- \parallel \vec{p}_1}^2 &= -\frac{4s^2}{q_2'^2 \vec{q}_2'^2} \cdot \frac{1}{(1)(2')} \left\{ (1-x)^2 + (1-x_1)^2 \right. \\ &\quad \left. + \frac{32}{q_2'^2 \vec{q}_2'^2} \cdot \frac{1}{(1)(2')} [x_1(p_1 \tilde{p})(p_1 p_+) + x(p_+ \tilde{p})(q_1 p_1)]^2 \right\}, \end{aligned} \quad (34)$$

where

$$\begin{aligned}\tilde{p} &= p_- - x_2 p_1, & q_2^{\prime 2} &= (p_1 - p_-)^2, \\ (2') &= -2(p_1 q_1)(1 - x_2), & (1) &= -2(p_1 p_+)(1 - x_2).\end{aligned}$$

The integration of the matrix element over $(p_+^\perp)^2$ and $(p_-^\perp)^2$ leads to the differential cross-section

$$\begin{aligned}d\sigma_{\tilde{p}-\|\tilde{p}_1} &= \frac{\alpha}{4\pi} L dx dx_2 \frac{d(q_2^\perp)^2}{(q_2^\perp)^2} \cdot \frac{d(q_1^\perp)^2}{(q_1^\perp)^2} \\ &\times \frac{d\phi}{2\pi} \cdot \frac{1}{(q_1^\perp + q_2^\perp)^2} \left[\frac{(1-x)^2 + (1-x_1)^2}{(1-x_2)^2} - \frac{4xx_1x_2}{(1-x_2)^4} \right].\end{aligned}\quad (35)$$

The restriction due to the exclusion of the collinear region when the created pair flies inside a narrow cone along the initial electron has the form:

$$\frac{|p_+^\perp|}{\varepsilon_1} > \theta_0, \quad p_+^\perp + q_1^\perp + q_2^\perp = 0, \quad (36)$$

or

$$\begin{cases} 1 > \cos \phi > -1 + \frac{\lambda^2 x_1^2 - (\sqrt{z_1} - \sqrt{z_2})^2}{2\sqrt{z_1 z_2}}, & |\sqrt{z_1} - \sqrt{z_2}| < \lambda x_1, \\ 1 > \cos \phi > -1, & |\sqrt{z_1} - \sqrt{z_2}| > \lambda x_1. \end{cases}\quad (37)$$

The integration of the differential cross-section (35) over the region defined in eq. (37) leads to

$$\begin{aligned}\sigma_{\tilde{p}-\|\tilde{p}_1} &= \frac{\alpha^4}{\pi Q_1^2} \mathcal{L} \int_1^{\rho^2} \frac{dz}{z^2} \int_{x_c}^{1-\Delta} dx \int_0^{1-x} dx_2 \left[\frac{(1-x)^2 + (1-x_1)^2}{(1-x_2)^2} \right. \\ &\left. - \frac{4xx_1x_2}{(1-x_2)^2} \right] \left\{ \Theta \ln \frac{z}{\lambda^2} + \Theta \ln \frac{(x^2 \rho^2 - z)^2}{x_1^2 x^4 \rho^4} + \ln \left| \frac{\rho^2(z - x^2)}{z - x^2 \rho^2} \right| \right\}.\end{aligned}\quad (38)$$

The total contribution of the semi-collinear kinematics to the cross-section is the sum of eqs. (28), (33), and (38):

$$\sigma_{\text{s-coll}} = \sigma_{\tilde{p}_+\|\tilde{p}_-} + \sigma_{\tilde{p}_+\|\tilde{q}_1} + \sigma_{\tilde{p}_-\|\tilde{p}_1}. \quad (39)$$

4 The Total Contribution Due to the Real and Virtual Pair Production

In order to obtain finite expression for the cross-section we have to add to eq. (39) the contribution of the collinear kinematics region (eq. (15)) as well

as the ones due to the production of virtual and soft pairs. Taking into account the leading and next-to-leading terms we can write the full hard pair contribution in the following form:

$$\begin{aligned}
\sigma_{\text{hard}} &= \frac{\alpha^4}{\pi Q_1^2} \int_1^{\rho^2} \frac{dz}{z^2} \int_{x_c}^{1-\Delta} dx \left\{ L^2 R(x) + \mathcal{L}[\Theta f(x) + f_1(x)] \right. \\
&+ \mathcal{L} \int_0^{1-x} dx_2 \left[\left(\Theta \ln \frac{(x^2 \rho^2 - z)^2}{x^2} + \ln \left| \frac{(z - x^2)(\rho^2 - z)(z - 1)x^2}{z - x^2 \rho^2} \right| \right) \varphi \right. \\
&- (\Theta \ln(x \rho^2 - z)^2 + \ln(z - x)^2) \varphi(x, x_2) \\
&\left. \left. - (\Theta \ln(x_1^2 x^2 \rho^4) + \ln x_2^2) \varphi(x_2, x) \right] \right\}, \quad L = \ln \frac{Q_1^2 z}{m^2}, \quad \mathcal{L} = \ln \frac{Q_1^2}{m^2},
\end{aligned} \tag{40}$$

where

$$\begin{aligned}
\varphi &= \varphi(x, x_2) + \varphi(x_2, x), \\
\varphi(x_2, x) &= \frac{(1-x)^2 + (x+x_2)^2}{(1-x_2)^2} - \frac{4xx_2(1-x-x_2)}{(1-x_2)^4}, \\
R(x) &= \frac{1}{3} \cdot \frac{1+x^2}{1-x} + \frac{1-x}{6x} (4 + 7x + 4x^2) + (1+x) \ln x.
\end{aligned}$$

Integrating over x_2 in the right-hand side of eq. (40) we obtain the final expression for the cross-section of hard pair production at small angle electron-positron scattering:

$$\begin{aligned}
\sigma_{\text{hard}} &= \frac{\alpha^4}{\pi Q_1^2} \int_1^{\rho^2} \frac{dz}{z^2} \int_{x_c}^{1-\Delta} dx \left\{ L^2 (1 + \Theta) R(x) + \mathcal{L}[\Theta F_1(x) + F_2(x)] \right\}, \\
F_1(x) &= d(x) + C_1(x), \quad F_2(x) = d(x) + C_2(x), \\
d(x) &= \frac{1}{1-x} \left(\frac{8}{3} \ln(1-x) - \frac{20}{9} \right), \\
C_1(x) &= -\frac{113}{9} + \frac{142}{9}x - \frac{2}{3}x^2 - \frac{4}{3x} - \frac{4}{3}(1+x) \ln(1-x) \\
&+ \frac{2}{3} \cdot \frac{1+x^2}{1-x} \left[\ln \frac{(x^2 \rho^2 - z)^2}{(x \rho^2 - z)^2} - 3\text{Li}_2(1-x) \right] + (8x^2 + 3x - 9 - \frac{8}{x} \\
&- \frac{7}{1-x}) \ln x + \frac{2(5x^2 - 6)}{1-x} \ln^2 x + \beta(x) \ln \frac{(x^2 \rho^2 - z)^2}{\rho^4}, \\
C_2(x) &= -\frac{122}{9} + \frac{133}{9}x + \frac{4}{3}x^2 + \frac{2}{3x} - \frac{4}{3}(1+x) \ln(1-x) \\
&+ \frac{2}{3} \cdot \frac{1+x^2}{1-x} \left[\ln \left| \frac{(z - x^2)(\rho^2 - z)(z - 1)}{(x^2 \rho^2 - z)(z - x)^2} \right| + 3\text{Li}_2(1-x) \right]
\end{aligned} \tag{41}$$

$$\begin{aligned}
& + \frac{1}{3}(-8x^2 - 32x - 20 + \frac{13}{1-x} + \frac{8}{x}) \ln x + 3(1+x) \ln^2 x \\
& + \beta(x) \ln \left| \frac{(z-x^2)(\rho^2-z)(z-1)}{x^2\rho^2-z} \right|, \quad \beta = 2R(x) - \frac{2}{3} \cdot \frac{1+x^2}{1-x}.
\end{aligned}$$

Formula (41) describes the small angle high energy cross-section of process (1) in the case where the created hard pair flies along the direction of the initial electron three-momentum, and we now have to double σ_H to take into account the production of a hard pair flying along the direction of the initial positron beam.

In order to pick out the dependence on the parameter Δ in σ_H we will use the following relation:

$$\begin{aligned}
\int_1^{\rho^2} dz \int_{x_c}^{1-\Delta} dx \Theta(x^2\rho^2 - z) &= \int_1^{\rho^2} dz \left[\int_{x_c}^{1-\Delta} dx - \int_{x_c}^1 dx \bar{\Theta} \right], \\
\bar{\Theta} &= 1 - \Theta(x^2\rho^2 - z).
\end{aligned} \tag{42}$$

Therefore

$$\int_1^{\rho^2} dz \int_{x_c}^{1-\Delta} \Theta \frac{dx}{1-x} = \int_1^{\rho^2} dz \left[\ln \frac{1-x_c}{\Delta} - \int_{x_c}^1 \frac{dx}{1-x} \bar{\Theta} \right], \tag{43}$$

$$\begin{aligned}
\int_1^{\rho^2} dz \int_{x_c}^{1-\Delta} dx \Theta \frac{\ln(1-x)}{1-x} &= \int_1^{\rho^2} dz \left[\frac{1}{2} \ln^2(1-x_c) - \frac{1}{2} \ln^2 \Delta \right] \\
&- \int_{x_c}^1 dx \frac{\ln(1-x)}{1-x} \bar{\Theta}.
\end{aligned} \tag{44}$$

The contribution to the cross-section of the small-angle Bhabha scattering connected with real soft (with an energy less than $\Delta \cdot \varepsilon$) and virtual pair production is defined [2] by the formula:

$$\begin{aligned}
\sigma_{\text{soft+virt}} &= \frac{4\alpha^4}{\pi Q_1^2} \int_1^{\rho^2} \frac{dz}{z^2} \left\{ L^2 \left(\frac{2}{3} \ln \Delta + \frac{1}{2} \right) + \mathcal{L} \left(-\frac{17}{6} + \frac{4}{3} \ln^2 \Delta \right) \right. \\
&\quad \left. - \frac{20}{9} \ln \Delta - \frac{4}{3} \zeta_2 \right\}.
\end{aligned} \tag{45}$$

Using eqs. (43) and (44) one can check that the auxiliary parameter Δ is cancelled in the sum $\sigma_{\text{tot}} = 2\sigma_{\text{hard}} + \sigma_{\text{soft+virt}}$, and we can write the total

contribution σ_{tot} as follows:

$$\begin{aligned} \sigma_{\text{tot}} = & \frac{2\alpha^4}{\pi Q_1^2} \int_1^{\rho^2} \frac{dz}{z^2} \left\{ L^2 \left(1 + \frac{4}{3} \ln(1-x_c) - \frac{2}{3} \int_{x_c}^1 \frac{dx}{1-x} \bar{\Theta} \right) + \mathcal{L} \left[-\frac{17}{3} \right. \right. \\ & \left. \left. - \frac{8}{3} \zeta_2 - \frac{40}{9} \ln(1-x_c) + \frac{8}{3} \ln^2(1-x_c) + \int_{x_c}^1 \frac{dx}{1-x} \bar{\Theta} \cdot \left(\frac{20}{9} - \frac{8}{3} \ln(1-x) \right) \right] \right. \\ & \left. + \int_{x_c}^1 dx [L^2(1+\Theta)\bar{R}(x) + \mathcal{L}(\Theta C_1(x) + C_2(x))] \right\}, \quad \bar{R}(x) = R(x) - \frac{2}{3(1-x)}. \end{aligned} \quad (46)$$

The right-hand side of eq. (46) is the master expression for the small-angle Bhabha scattering cross-section connected with the pair production. It is finite and could be used for numerical estimates. Note that the leading term is described by the electron structure function $D_e^{\bar{e}}(x)$, which represents the probability to find a positron inside an electron with virtuality Q^2 provided that the electron loses the energy part $(1-x)$ [9].

In table 1 we present the ratio of the RC contribution due to the pair production σ_{tot} (46) to the normalization cross-section σ_0 ,

$$\sigma_0 = \frac{4\pi\alpha^2}{\varepsilon^2\theta_{\min}^2}. \quad (47)$$

In table 2 we illustrate the comparison between the non-leading contribution (containing $\mathcal{L}^1 = \ln Q_1^2/m^2$) and the total one (containing \mathcal{L}^2 and \mathcal{L}^1).

Table 1. The ratio $S = \sigma_{\text{tot}}/\sigma_0$ in percents, as a function of x_c , for NN ($\rho = 1.74$, $\theta_{\min} = 1.61$ rad) and WW ($\rho = 2.10$, $\theta_{\min} = 1.50$ rad) counters, $\sqrt{s} = 2\varepsilon = M_Z = 91.187$ GeV.

x_c	0.2	0.3	0.4	0.5	0.6	0.7	0.8
$S_{NN}, \%$	-0.018	-0.022	-0.026	-0.029	-0.033	-0.038	-0.046
$S_{WW}, \%$	-0.013	-0.019	-0.024	-0.029	-0.035	-0.042	-0.052

Table 2. Values of R_{NN} and R_{WW} as functions of x_c , where R represents the ratio of the non-leading contribution in eq. (46) with respect to the total one, for NN and WW counters.

x_c	0.2	0.3	0.4	0.5	0.6	0.7	0.8
R_{NN}	0.036	-0.122	-0.194	-0.238	-0.268	-0.335	-0.465
R_{WW}	0.179	-0.021	-0.088	-0.120	-0.179	-0.271	-0.415

5 Conclusions

The result derived in this paper combined with those derived earlier in [4,5,6] thus give the full analytical description of the small angle electron–positron scattering cross-section at LEP I energies with one and two photon radiation as well as pair production. The description takes into account the leading and next-to-leading logarithmic approximations and gives the possibility to describe the cross-section with an accuracy not worse than 0.1% provided that the scattered electron and positron are recorded by symmetrical circular detectors. By using the above derivation it is possible to carry out the calculations also for non-symmetrical detectors.

Numerical calculations of the virtual and real pair production RC contributions show their compensation at the level of $10^{-3}\%$ for the given angular apertures and x_c range. Table 2 shows that the next-to-leading contribution is comparable with the leading one. Their ratio is sensitive to x_c and angle ranges.

We note that, in a realistic case, one has to take into account the fact that detectors cannot distinguish a single particle event from the one when two or more particles hit the same point of the detector simultaneously. In that case the obtained results could be easily changed: starting from the presented differential cross-sections the integration must be done by imposing experimental restrictions.

We want also to emphasize that the method and some of the derived results could be used for calculating radiative corrections to deep inelastic scattering as well as for cross-sections of some normalization processes at HERA. We hope to consider these questions in a future publication.

Acknowledgements

We are grateful to V.A. Fadin and L.N. Lipatov for fruitful discussions and criticism. This work is supported in part by INTAS grant 93–1867.

Appendix A

We give here a list of the relevant integrals for the collinear kinematical region, calculated within the logarithmic accuracy. The definitions of eq. (9) are used. We imply, in the left-hand side of the relations below the general operation:

$$\langle\langle(\dots)\rangle\rangle \equiv \int_0^{z_0} dz_1 \int_0^{z_0} dz_2 \int_0^{2\pi} \frac{d\phi}{2\pi} (\dots), \quad (\text{A.1})$$

and suggest $z_0 = (\varepsilon\theta_0/m)^2 \gg 1$, $L_0 = \ln z_0 \gg 1$. The details of the calculations can be found in the Appendix of paper [5]. The results are:

$$\begin{aligned}
\left\langle \left(\frac{x_2 D + (1-x_2)A}{DC} \right)^2 \right\rangle &= \frac{L_0}{(1-x_2)^2} \left\{ L_0 + 2 \ln \frac{x_1 x_2}{x} - 8 \right. \\
&\quad \left. + \frac{(1-x)^2(1-x_2)^2}{xx_1x_2} \right\}, \quad \left\langle \frac{1}{DC} \right\rangle = \frac{L_0}{x_1x_2(1-x_2)} \left[\frac{1}{2}L_0 + \ln \frac{x_1x_2}{x} \right], \\
\left\langle \left(\frac{x_2 A_1 - x_1 A_2}{AD} \right)^2 \right\rangle &= \frac{L_0}{(1-x)^2} \left\{ L_0 + 2 \ln \frac{x_1 x_2}{x} - 8 + \frac{(1-x)^2}{xx_1x_2} - \frac{4(1-x)}{x} \right\}, \\
\left\langle \frac{x_1 A_2 - x_2 A_1}{AD^2} \right\rangle &= \frac{(x_1 - x_2)L_0}{xx_1x_2(1-x)}, \quad \left\langle \frac{1}{D^2} \right\rangle = \frac{L_0}{xx_1x_2}, \\
\left\langle \frac{1}{AD} \right\rangle &= \frac{-L_0}{x_1x_2(1-x)} \left[\frac{1}{2}L_0 + \ln \frac{x_1x_2}{x} \right], \quad \left\langle \frac{1}{C^2 D} \right\rangle = \frac{-L_0}{x_1(1-x_2)^3}, \\
\left\langle \frac{1}{AC} \right\rangle &= \frac{-L_0}{x_1x_2^2} \left[L_0 + 2 \ln \frac{x_1x_2}{x} + 2 \ln \frac{xx_2}{(1-x)(1-x_2)} \right], \quad \left\langle \frac{1}{A^2 D} \right\rangle = \frac{-L_0}{(1-x)^3}, \\
\left\langle \frac{A}{C^2 D^2} \right\rangle &= \frac{x_2 L_0}{x_1(1-x_2)^4}, \quad \left\langle \frac{C}{A^2 D^2} \right\rangle = \frac{-x_2 L_0}{(1-x)^4}, \\
\left\langle \frac{A}{CD^2} \right\rangle &= \frac{-L_0}{x_1(1-x_2)^2} \left[\frac{1}{2}L_0 + \ln \frac{x_1x_2}{x} \right] + L_0 \frac{x_2x - x_1}{xx_1x_2(1-x_2)^2}, \\
\left\langle \frac{C}{AD^2} \right\rangle &= \frac{-L_0}{x_1(1-x)^2} \left[\frac{1}{2}L_0 + \ln \frac{x_1x_2}{x} \right] - L_0 \left(\frac{x_1 - x_2}{x_1x_2(1-x)^2} + \frac{1}{xx_2(1-x)} \right).
\end{aligned} \tag{A.2}$$

Appendix B

Here we derive eq. (28), starting from eq. (38), by integration over regions (26) and (26), taking into account the aperture of the detectors. Let us note first that

$$\begin{aligned}
\frac{d(q_2^\perp)^2}{(q_2^\perp)^2} \cdot \frac{d(q_1^\perp)^2}{(q_1^\perp + q_2^\perp)^2} \cdot \frac{d\phi}{2\pi(q_1^\perp + xq_2^\perp)^2} &= \frac{1}{Q_1^2} \cdot \frac{dz_2}{z_2} \cdot \frac{dz_1 d\phi}{2\pi(1-x)(z_2x - z_1)} \\
&\cdot \left[-\frac{1}{z_1 + z_2 + 2\sqrt{z_1z_2} \cos \phi} + \frac{1}{(z_1/x) + xz_2 + 2\sqrt{z_1z_2} \cos \phi} \right]. \tag{B.1}
\end{aligned}$$

Integrating the right-hand side of eq. (B.1) we have to keep in mind that the first term in the brackets is sensitive to region (26) and the second to region (26). The aperture of the symmetrical circular detector is shown in fig. 3.

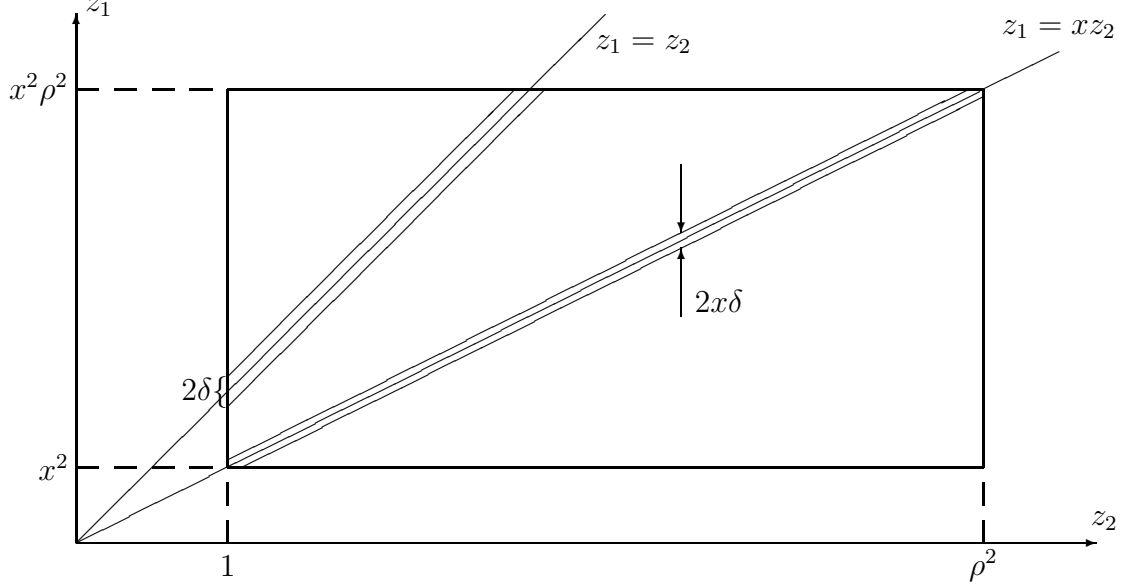


Fig. 3. The aperture of the symmetrical circular detector for the integration over z_1 and z_2 in the case when only the initial electron loses energy for the pair creation; $\delta = 2\sqrt{z_2}\lambda(1-x)$.

We present in detail only the integration of the first term in the brackets in the right-hand side of eq. (B.1). If $|\sqrt{z_1} - \sqrt{z_2}| < \lambda(1-x)$ then the angular integration gives

$$\begin{aligned} \frac{1}{2\pi} \int \frac{d\phi}{z_1 + z_2 + 2\sqrt{z_1 z_2} \cos \phi} &= \frac{2}{\pi} \int_0^{\phi_{\max}} \frac{d\phi}{z_1 + z_2 + 2\sqrt{z_1 z_2} \cos \phi} \quad (\text{B.2}) \\ &= \frac{2}{\pi\sqrt{a^2 - b^2}} \arctan \left(\frac{a - b}{\sqrt{a^2 - b^2}} \tan \frac{\phi}{2} \right) \Big|_0^{\phi_{\max}}, \end{aligned}$$

where

$$\begin{aligned} \phi_{\max} &= \arccos \left(-1 + \frac{\lambda^2(1-x)^2 - (\sqrt{z_1} - \sqrt{z_2})^2}{2\sqrt{z_1 z_2}} \right), \\ a &= z_1 + z_2, \quad b = 2\sqrt{z_1 z_2}. \end{aligned}$$

Because of the smallness of the values $\lambda^2(1-x)^2$ and $|\sqrt{z_1} - \sqrt{z_2}|$ with respect to z_1 and z_2 , we can rewrite the last term in eq. (B.2) in the following form:

$$J = \frac{1}{\pi} \cdot \frac{1}{\sqrt{z_2} |\sqrt{z_1} - \sqrt{z_2}|} \arctan \frac{|\sqrt{z_1} - \sqrt{z_2}|}{\sqrt{\lambda^2(1-x)^2 - (\sqrt{z_1} - \sqrt{z_2})^2}}. \quad (\text{B.3})$$

Let $z_2 > z_1$, then in the region under consideration we have $\sqrt{z_1} > \sqrt{z_2} - \lambda(1-x)$, and we can carry out the subsequent integration over z_1 in eq. (B.1) by taking $z_1 = z_2$ in the factor $(xz_2 - z_1)^{-1}$ and introducing the new variable $t = \lambda(1-x)(\sqrt{z_2} - \sqrt{z_1})$ in J . Thus we obtain:

$$J = 2 \frac{2}{\pi} \int_0^1 \frac{dt}{t} \arctan \frac{t}{\sqrt{1-t^2}} = 2 \ln 2, \quad (\text{B.4})$$

where the additional factor 2 is due to the contribution when $z_1 > z_2$. From fig. 3 we see that the region $|\sqrt{z_1} - \sqrt{z_2}| < \lambda(1-x)$ contributes only if $z_2 < x^2 \rho^2$. That is why we have to write the contribution corresponding to $|\sqrt{z_1} - \sqrt{z_2}| < \lambda(1-x)$ in eq. (B.1) as:

$$\frac{1}{Q_1^2} \int_1^{\rho^2} \frac{dz_2}{z_2^2} \frac{1}{(1-x)^2} 2\Theta \ln 2, \quad \Theta = \Theta(x^2 \rho^2 - z_2). \quad (\text{B.5})$$

If now $|\sqrt{z_1} - \sqrt{z_2}| > \lambda(1-x)$ the angular integration is trivial and the subsequent integration over z_1 and z_2 is reduced to the integration of the function $\{(z_1 - xz_2)|z_1 - z_2|\}^{-1}$ over the rectangle $1 < z_2 < \rho^2$, $x^2 < z_1 < x^2 \rho^2$ without the narrow strip of width 2δ ($\delta = 2\sqrt{z_2}\lambda(1-x)$). The result reads:

$$\frac{1}{Q_1^2} \int_1^{\rho^2} \frac{dz_2}{z_2^2} \frac{1}{(1-x)^2} \left\{ \ln \left| \frac{(z_1 - x^2)(x\rho^2 - z_2)}{(x - z_2)(z_2 - x^2\rho^2)} \right| + \Theta \left(-2 \ln 2 \right. \right. \quad (\text{B.6}) \\ \left. \left. + \ln \frac{(x^2\rho^2 - z_2)^2}{(x\rho^2 - z_2)^2 x^2} \right) \right\}.$$

It is easy to see that the full contribution of the first term in brackets in eq. (B.1) is reduced to eq. (B.6) without $-2\Theta \ln 2$ in the latter.

The integration of the second term in brackets in eq. (B.1) can be done in full analogy. The result could be written as:

$$\frac{1}{Q_1^2} \int_1^{\rho^2} \frac{dz_2}{z_2^2} \frac{1}{(1-x)^2} \left\{ \ln \frac{z_2}{\lambda^2} + \ln \left| \frac{(\rho^2 - z_2)(z_2 - 1)}{(x - z_2)(z_2 - x\rho^2)} \right| \right\}, \quad (\text{B.7})$$

and formula (28) becomes obvious.

References

- [1] B. Pietrzyk, preprint LAPP-EXP-94.18, Invited talk at the Conference on "Radiative Corrections: Status and Outlook", Gatlinburg, TN, USA, 1994, to be published in the Proceedings.

- [2] O. Adriani, M. Aguilar–Benitez et al., Phys. Reports C **236**, 1 (1993).
- [3] S. Jadach et al., Phys. Lett. B, **268**, 253 (1991); Comput. Phys. Commun. **70**, 305 (1992);
M. Cacciari, A. Deandrea, G. Montagna, O. Nicosini and L. Trentadue, Phys. Lett. B **271**, 431 (1991);
W. Beenakker and B. Pietrzyk, Phys. Lett. B **296**, 241 (1992); *ibid.* **304**, 687 (1988);
D. Bardin, W. Hollik and T. Riemann, preprints MPI-PAE/Pth 32/90, PHE90-9;
M. Böhm, A. Denner and W. Hollik, Nucl. Phys. B **304**, 687 (1988);
W. Beenakker, F.A. Berends and S.C. van der Marck, Nucl. Phys. B **355**, 281 (1991);
M. Caffo, H. Czyz and E. Remiddi, Nuovo Cimento A **105**, 277 (1992).
- [4] A.B. Arbuzov, V.S. Fadin, E.A. Kuraev, L. Lipatov, N. Merenkov and L. Trentadue, in "Reports of the working group on precision calculations for the Z resonance", eds. D. Bardin, W. Hollik and G. Passarino, Report CERN 95-03, March 1995, p.369.
- [5] N.P. Merenkov, Sov. J. Nucl. Phys. **48**, 1073 (1988).
- [6] N.P. Merenkov, Sov. J. Nucl. Phys. **50**, 469 (1989).
- [7] V.N. Baier, V.S. Fadin, V.A. Khoze and E. Kuraev, Phys. Reports C **78**, 293 (1982);
V.M. Budnev, I.F. Ginzburg, G.V. Meledin et al., Phys. Reports C **15**, 183 (1975).
- [8] J.C. Collins, D.E. Soper, G. Sterman, in *Perturbative QCD*, ed. by A.H. Mueller, (World Scientific Pub., 1989);
V.N. Baier, V.S. Fadin and V.A. Khoze, Nucl. Phys. B **65**, 381 (1973).
- [9] E.A. Kuraev, N.P. Merenkov and V.S. Fadin, Sov. J. Nucl. Phys. **47**, 1009 (1988);
M. Skrzypek, Acta Phys. Polon. B, **23**, 135 (1992).